



저작자표시-비영리-변경금지 2.0 대한민국

이용자는 아래의 조건을 따르는 경우에 한하여 자유롭게

- 이 저작물을 복제, 배포, 전송, 전시, 공연 및 방송할 수 있습니다.

다음과 같은 조건을 따라야 합니다:



저작자표시. 귀하는 원저작자를 표시하여야 합니다.



비영리. 귀하는 이 저작물을 영리 목적으로 이용할 수 없습니다.



변경금지. 귀하는 이 저작물을 개작, 변형 또는 가공할 수 없습니다.

- 귀하는, 이 저작물의 재이용이나 배포의 경우, 이 저작물에 적용된 이용허락조건을 명확하게 나타내어야 합니다.
- 저작권자로부터 별도의 허가를 받으면 이러한 조건들은 적용되지 않습니다.

저작권법에 따른 이용자의 권리는 위의 내용에 의하여 영향을 받지 않습니다.

이것은 [이용허락규약\(Legal Code\)](#)을 이해하기 쉽게 요약한 것입니다.

[Disclaimer](#)

Master of Science degree

**TLQP-21 improves microglial β -Amyloid
phagocytosis via interaction with C3a receptor
(C3AR1)**

**TLQP-21 의 미세아교세포 C3a 수용체 (C3AR1)를 매개로
한 베타-아밀로이드 섭취의 촉진**

**The Graduate School
of the University of Ulsan**

Department of Medicine

You-Jin Jang

**TLQP-21 improves microglial β -Amyloid
phagocytosis via interaction with C3a receptor
(C3AR1)**

Supervisor Dong-Hou Kim

Master's thesis

**Submitted to
The Graduate School of the University of Ulsan
In partial Fulfillment of the Requirements
For the Degree of**

Master of Science

by

You-Jin Jang

**Department of Medicine
Ulsan, Korea
February 2018**

**TLQP-21 improves microglial β -Amyloid
phagocytosis via interaction with C3a receptor
(C3AR1)**

This certifies that the master's thesis of
You-Jin Jang is approved.

Committee Chair Dr.

Seung-Yong Yoon

Committee Member Dr.

Han Choe

Committee Member Dr.

Dong-Hou Kim

**Department of Medicine
Ulsan, Korea
February 2018**

Abstract

TLQP-21 improves microglial β -Amyloid phagocytosis via interaction with C3a receptor (C3AR1)

The Graduate School of the University of Ulsan College of Medicine

You-Jin Jang

In Alzheimer's disease (AD), β -amyloid ($A\beta$) plaque is caused by overproduction and impaired clearance of $A\beta$ by glial cells including microglia and astrocytes. Because microglia play important protective role in the central nervous system (CNS), there have been many tries to find effective agents for improving microglial $A\beta$ phagocytosis. VGF (VGF nerve growth factor inducible), the neuropeptide belongs to granin family, is a precursor protein that cleaved to several VGF-derived peptides by proteolytic enzymes and TLQP-21 increases intracellular Ca^{2+} levels on microglia, suggesting that TLQP-21 can modulate microglial function via stimulation of intracellular signaling. However, whether TLQP-21 modulates microglial function and pathogenesis of AD or not is unclear.

In this study, it's confirmed that TLQP-21 improves phagocytosis and promotes $fA\beta$ uptake via C3AR1-dependent mechanism on microglial BV2 cell lines. TLQP-21 also stimulates $A\beta$ degradation by enhancing the function of autophagosome and lysosome, and consequently enhances the ability of $fA\beta$ clearance on microglia. Despite of these effects, TLQP-21 did not affect inflammation-related cytokines release. These results suggest that TLQP-21 induced microglial $A\beta$ clearance and TLQP-21 may be novel potential therapeutics for AD.

Keywords: Alzheimer's disease, VGF, TLQP-21, microglia, $A\beta$, clearance

Contents

Abstracts	i
Contents	ii
List of figures	iii
Introduction	1
Materials and Methods	6
1. Reagents	
2. Microglial BV2 cell culture	
3. LDH cell cytotoxicity assay	
4. MTT cell viability assay	
5. Microglial phagocytosis	
6. Flow cytometry	
7. Western blot	
8. Immunocytochemistry	
9. siRNA Transfection	
10. Real Time – quantitative PCR	
Results	11
1. TLQP-21 enhances microglial phagocytic activity.	
2. TLQP-21 increases fA β uptake on microglial BV2 cells.	
3. C3AR1 is associated with TLQP-21-mediated A β uptake.	
4. TLQP-21 improves microglial A β clearance.	
5. TLQP-21 degrades engulfed A β via stimulation of lysosomal degradation pathway.	
6. TLQP-21 has no effect on inflammation-related cytokines release.	
Discussion	27
References	31
Abstract in Korean	39

List of Figures

Figure 1. Scheme of VGF precursor protein sequences indicated cleavage sites.	5
Figure 2. VGF-derived peptides are not toxic to microglial BV2 cell lines.	13
Figure 3. TLQP-21 enhances microglial phagocytic activity.	14
Figure 4. TLQP-21 increases intracellular A β protein levels on microglial BV2 cell lines.	16
Figure 5. C3AR1 treatment antagonist attenuates TLQP-21-mediated microglial fA β phagocytosis.	17
Figure 6. siC3AR1 transfection attenuates TLQP-21-mediated microglial fA β phagocytosis.	18
Figure 7. TLQP-21 promotes microglial A β degradation overtime.	21
Figure 8. TLQP-21-treated microglial BV2 cultures more degrades engulfed A β	22
Figure 9. Lysosomal degradation pathway is related to TLQP-21-mediated microglial A β degradation.	23
Figure 10. TLQP-21 stimulates lysosomal degradation pathway.	24
Figure 11. TLQP-21 shows no change on release of inflammation-related cytokines. ...	26
Figure 12. Propose model of TLQP-21 functions in the microglial A β clearance.	30

Introduction

Alzheimer's disease is the most common form of dementia, and 60 to 70% of demented patients are classified as having AD¹. During the illness progresses, the patients gradually lose bodily function as they have the synapse loss, cognitive impairment and memory decline like symptoms of general dementia²⁻⁴. This disease was announced in 1906 by German psychiatrist Alois Alzheimer⁵. In most cases, AD occurs more than 65 years of age, but rarely before it can develop⁶. In United States, about 19% of the population aged 75 to 84, and 42% of the population aged 85 or older suffer from the disease in 2000⁷. In 2006, there were 26,600,000 AD patients worldwide and in 2050, one out of every 85 person are expected to develop AD⁸. In some of the early-onset AD termed familiar AD, autosomal dominant fashion of genetic mutations at amyloid precursor protein (APP), presenilin 1 (PS-1) and PS-2 genes is inherited⁹⁻¹¹. On the contrary, the late-onset AD may be caused by non-dominant factors and environment and apolipoprotein E4 (ApoE4) is a major risk factor for late-onset AD^{9, 12-13}. Genetic risk factors associated with late onset AD have been gradually revealed¹⁴.

In the brain of AD patients, the neuron cells are extinct, the brain is shrunken, ventricles are enlarged, and neurofibrillary tangles (NFTs) in neurons and extracellular senile plaques known as the most typical pathological changes are observed¹⁵⁻¹⁷. NFTs have a pivotal role in the progression of AD and are formed by aggregation of hyperphosphorylated microtubule-associated protein tau¹⁸. Tau is present in the axons of neurons, helps to stabilize microtubules, and regulates axonal transport. The tau protein undergoes several types of post translational modification (PTM), including phosphorylation and acetylation. When the phosphorylation of tau is excessive, hyperphosphorylated tau forms self-assembly with tangles of paired helical filaments (PHFs)¹⁸⁻¹⁹. The binding affinity of hyperphosphorylated tau protein and microtubule is weakened, resulting in destabilizing the cytoskeleton and this eventually leads to the deterioration of neuronal functions¹⁸.

Senile plaques, the other major pathological finding in AD, are formed by the accumulation of A β in the gray matter of the brain and A β peptides are generated from the APP. APP, Type-I transmembrane protein²⁰, is produced in neurons and has various

functions including cell adhesion²¹⁾, neurite outgrowth²¹⁻²²⁾, synaptogenesis^{21, 23)} and axonal trafficking of neuronal proteins^{21, 24)}. APP undergoes anterograde axonal transport after being transferred from ER or Golgi²⁵⁻²⁷⁾ and can be truncated by α -secretase and γ -secretase or by β -secretase and γ -secretase after being transported to the cell surface²⁰⁾. β -secretase cleaves the amino acids of APP corresponding to N-terminal end of A β , results in producing secreted sAPP β and the remaining part attached to the membrane called CTF β ²⁸⁾. Sequentially, A β is formed as CTF β is cleaved again by γ -secretase. The A β , produced in the process of proteolyzing the APP, is released to the extracellular space and senile plaque can be formed when they are aggregated. In many studies, it has reported that toxicity of A β on neuron is mediated by a variety of mechanisms including synaptic dysfunction²⁹⁻³⁰⁾, mitochondrial dysfunction³¹⁾, inflammation³²⁾ and oxidative stress³³⁾.

Microglia, called the resident macrophages in the brain, senses the pathogens, damaged synapses or neuronal cells and host-derived ligands in the healthy CNS as a fundamental role. In this way, the type of insult is detected and consequently the innate adaptive immune response is induced, thereby controlling inflammation³⁴⁾. Microglial cells are easily observed around the senile plaque and remove A β deposits through several molecular mechanisms; first, microglial cells recognize plaque accumulation and migrate to nearby. They 'eat' A β through phagocytosis and micropinocytosis, receptor-mediated endocytosis and other processes³⁵⁻³⁷⁾. Finally, 'eaten' A β which is taken into phagosomes is processed by endosomal-lysosomal degradation pathway³⁸⁾.

In AD, function of microglia is degenerated as disease progress. These microglial cells exhibit a reactive phenotype characterized by the cell body being small, fat, and extending the ramified process. Microglia in AD has been shown functional impairment about ingestion and degradation of accumulated debris or inclusions and phagocytic impairment cause impairment of target detection and delay of migration on microglia, resulting in impairment of phagocytic mechanisms from the engulfment to endosomal-lysosomal pathway³⁹⁾.

VGF is first discovered as a gene transcriptionally regulated by NGF-treated PC12 cells⁴⁰⁾. This protein is the granin-related neuropeptide which expressed in hippocampus, cerebral cortex and hypothalamus⁴¹⁻⁴⁴⁾ and exclusively in neuron and neuroendocrine cells⁴¹⁾.

⁴⁵⁻⁴⁶). The VGF precursor protein of mouse is highly conserved mammalian polypeptides and has 615 amino acids sequences. It is cleaved with various bioactive peptides through proteolysis by several enzymes including prohormone convertase 1/3 (PC1/3) and prohormone convertase 2 (PC2)⁴⁶, as shown at Figure 1. In C-terminal of VGF precursor protein, PC2 produces NAPP129 and PC1/3 produces not only NAPP-129 like PC2 but also TLQP-62⁴⁷. In addition, TLQP-62 is cleaved with TLQP-21 and AQEE-30 and AQEE-30 sequentially can be further divided into AQEE-11 and LQEQ-19. Less commonly known than peptides derived from C-terminal of VGF precursor protein, peptides derived from N-terminal of VGF precursor include Neuroendocrine regulatory peptides such as NERP-1 and NERP-2 and also, peptides named NERP-3 and NERP-4 have also been recently discovered⁴⁸⁻⁴⁹. TPGH is independently produced in VGF424-434.

Each VGF-derived peptide has various specific function on central nervous system. NEPR-1 and NERP-2, belonging to neuroendocrine regulatory peptides (NERPs), has 25 amino acids and 38 amino acids corresponding to amino acids 285-309 and 310-347 of the VGF precursor protein, respectively. NERPs are expressed in the paraventricular nucleus and supraoptic nucleus and these proteins have been reported that they co-localized with the vasopressin and suppress its release from the hypothalamus⁵⁰. TLPQ-62 is the peptide produced by truncation of the C-terminal of VGF precursor protein. This peptide is known to function mainly in hippocampal neuron. In that region of brain, TLQP-62 enhances synaptic activity and neurogenesis⁵¹⁻⁵². TLQP-62 also modulates hippocampus-related behavior through a BDNF-dependent mechanism⁵³⁻⁵⁴. AQEE-30, AQEE-11, LQEQ-19 also play a role in various aspects of the function. AQEE-30 derived from the N-terminal of TLQP-62 peptides also regulate synaptic function as TLQP-62⁵⁵. AQEE-11 and LQEQ-19, fragments that are produced by truncating AQEE-30 induces penile erection⁵⁶.

TLQP-21 is derived from the C-terminal of the VGF precursor protein and this peptide is the most studied fragment of VGF-derived peptides. TLQP-21 regulates a number of molecular biologic mechanisms and behavioral patterns. TLQP-21 increases energy expenditure while reducing food intake and body weight in mice and Siberian hamster⁵⁷⁻⁵⁸. Similar to previous reports, TLQP-21 also inhibits obesity via enhancement of lipolysis⁵⁹⁻⁶⁰. TLQP-21, in addition, functions in conjunction with a stress response, pancreatic hormone

secretion or inflammatory pain. TLQP-21 has been reported to function as well as interacting receptors. TLQP-21 activates macrophage through interaction with gC1qR in rat, according to Chen et al., 2013⁶¹⁾ and C3AR1, the complement C3a receptor 1, also interacts with TLQP-21 in rodent cell lines⁶²⁻⁶³⁾.

Although VGF-derived peptides are decreased in CSF of AD patients⁶⁴⁾, the various changes caused by the reduction of these peptides in AD have not been disclosed. And VGF is a protein released from neurons, which will affect various glial cells. Therefore, I sought to deduce the effect of each VGF-derived peptide on AD pathology by the investigation the effects on microglia. Because TLQP-21 increases intracellular Ca^{2+} levels and this process results in activation of the Ca^{2+} -dependent K^{+} channels in microglia⁶⁵⁾, I also hypothesized that the function of TLQP-21 may affect the functional activity of microglia including microglial phagocytosis and releasing inflammation-related products. In this study, I demonstrated that TLQP-21 improves microglial $\text{A}\beta$ uptake through phagocytosis and interaction between TLQP-21 and C3AR1, the complement C3a receptor 1, is required to TLQP-21-mediated microglial $\text{A}\beta$ phagocytosis.

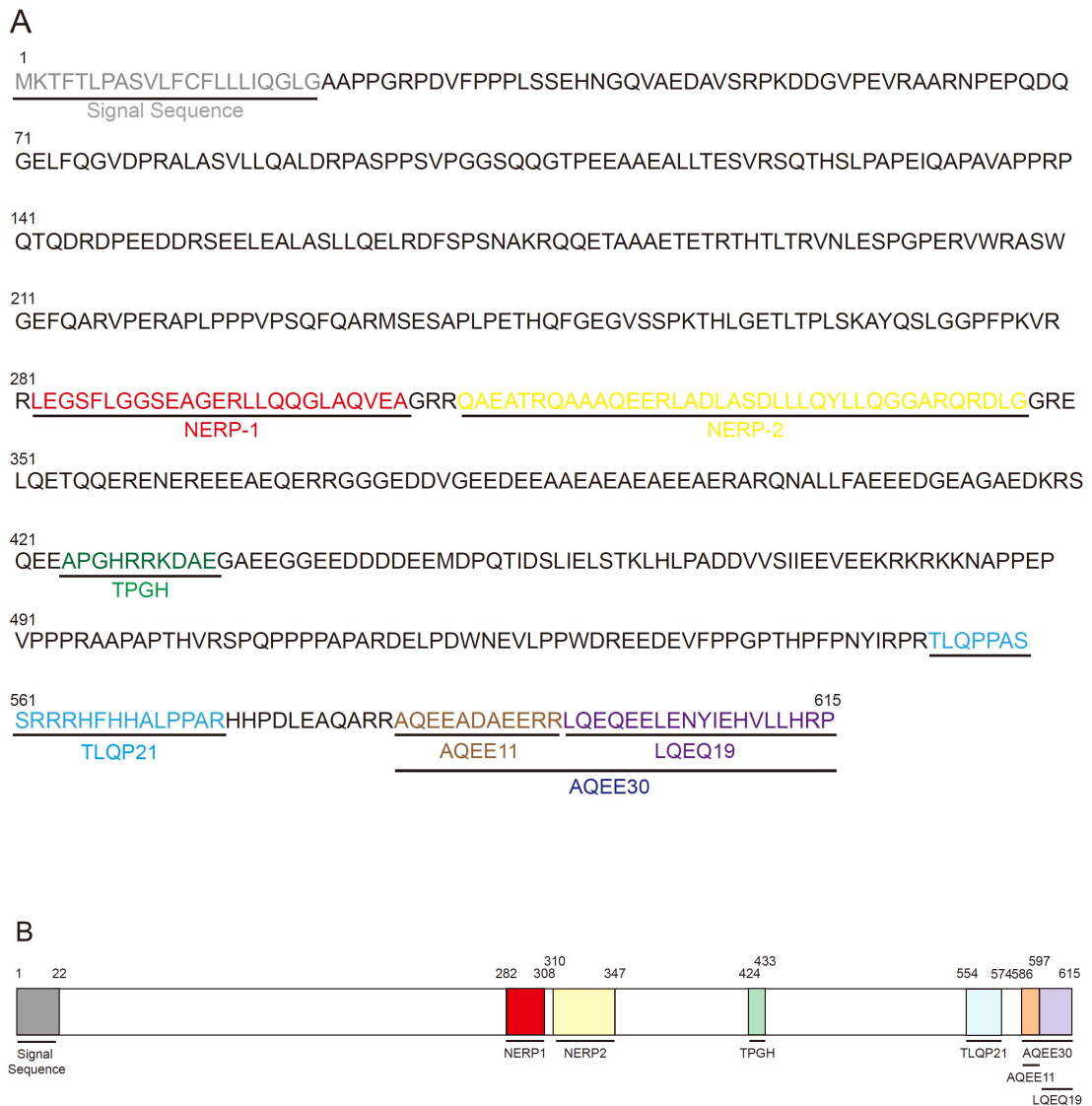


Figure 1. Scheme of VGF precursor protein sequences indicated cleavage sites.

(A) VGF precursor protein sequences in human and mouse indicated cleavage sites and VGF-derived peptides derived from VGF precursor protein. (B) Scheme of VGF-derived peptides on VGF precursor protein.

Materials & Methods

Reagents

VGF-derived peptides

Mouse TLQP-21 was synthesized and purchased from Genscript. TLQP-21 was dissolved in distilled water to 100 μ M and stored at -80 $^{\circ}$ C until use. TLQP-21 is derived from the C-terminal of VGF precursor protein and mouse TLQP-21 was used for this study because I used cell line of mouse species.

Fibril β -amyloid 1-42 or FITC-fibril β -amyloid 1-42

β -amyloid protein 1-42 (A β 1-42) or FITC- β -amyloid protein 1-42 (FITC-A β 1-42) were purchased from Bachem. Protein was dissolved in 0.5% NH₄OH to 500 μ M and stored at -80 $^{\circ}$ C. Fibril A β was made by incubation at 37 $^{\circ}$ C for 24hrs to final concentration 50 μ M.

C3AR1 antagonist

SB290157 was purchased from sigma and dissolved in D.W to 1mM. Drug stored at -20 $^{\circ}$ C until use.

Lipopolysaccharide (LPS)

LPS (Sigma, L2762-10MG) was dissolved in distilled water to 5mg/mL and stored at 4 $^{\circ}$ C until use.

Bafilomycin A1 (Baf.A1) and MG132

Baf.A1 and MG132 were purchased from sigma and calbiochem, respectively and dissolved in DMSO to 40 μ M and 5mM, respectively. These drugs stored at -20 $^{\circ}$ C until use.

Microglial BV2 cell lines culture

BV2 microglial cells were stocked with 20% DMSO, 10% fetal bovine serum (FBS, Gibco, 16000-044) and 1% PenStrep (Gibco, 15140.022) in Dulbecco's modified Eagle's medium (DMEM)/high glucose (Life Technologies, Inc., 21013024). The stocked cells diluted with DMEM containing 10% FBS and collected with centrifuging at 1000rpm for 2minutes to eliminate DMSO. These cells are cultured in 10cm dish with DMEM containing 10% FBS and 1% PenStrep. For experiments, 0.25% Trypsin-EDTA (Gibco, 25200-056) was used to cell dissociation to the dish and 2.4x10⁶ cells were seeded in plate. Microglial BV2

cells were sub-cultured and used until they reached 20 passages.

LDH cytotoxicity assay.

The cytotoxicity test was carried out using cell cytotoxicity kit (Progema, G1780). Cultured medium was transferred duplicate to 96well plates. The medium treated with LDH solution at final concentration 1mg/ml and incubated at room temperature for 30minutes in darkroom conditions and treated again with Stop solution to stop the function of LDH solution. Absorbance was measured in each well at 490nm with Magellan 3.0 system reader.

MTT cell viability assay

Cells were treated with MTT (Life Science, 19265) at final concentration 1mg/ml for 4hours. The cells were treated again with 100µl of DMSO to dissolve formazan after removed MTT-treated media. Within 30minutes after treatment with DMSO, the amount of formazan was measured at 570nm absorbance with a reference wavelength of 650nm using Magellan 3.0 system reader.

Microglial phagocytosis assay

Microglial phagocytosis assay was performed as previously report⁶⁶. Briefly, latex beads (Sigma, L1030) were diluted to 1:5 in FBS and incubated at 37°C for 1hour for preopsonization to induce microglial engulfment of artificial substrate. FBS containing beads was diluted with DMEM so that the final concentration of beads is 0.01 % (v/v) and microglial conditioned media were replaced with DMEM containing FBS and beads. Cultures were incubated at 37°C for 2hours at 5% CO₂ atmosphere.

Flow cytometry

For sampling, cells were washed two times with PBS and dissociated from PDL-coated wells with 200µL Trypsin-EDTA. The cells were suspended with 800µL DMEM with 10% FBS, centrifuged on 6000rpm for 2minutes and washed with PBS two times. After washed, the cells were suspended again with 300µL fixative (2% paraformaldehyde [PFA] in PBS, pH7.3) for flow cytometry and incubated on 4°C before calculating.

For calculating, Canto II was used for counting the number of living cells engulfing FITC-fibril A β . The total counted cells were fixed to 10,000 cells.

Western blot

Total proteins were extracted with 0.1% triton X-100 (Sigma, X100-100mL) 1x protease inhibitor cocktail and 1x phosphatase inhibitor in PBS (140mM NaCl, 10mM Na₂HOP₄, 1.75mM KH₂PO₄, pH7.4). The lysates were incubated at 4°C for 30minutes and debris was removed by centrifuging at 13000rpm for 30minute at 4°C. Amount of proteins was calculated with protein assay dye reagent (Bio-Rad, 500-0006) as manufacturer's instruction and equalized with the lysis buffer at the lowest density. Equal amounts of proteins were mixed with 4x SDS-PAGE loading buffer (1% SDS, 2.5% Glycerol, 0.5% β -mercaptoethanol, and bromophenol blue in 62.5mM Tris-HCl [pH6.8]) and stored at -20°C until use.

Proteins were separated on SDS-PAGE gel with Tris/Glycine/SDS buffer (Bio-Rad, 161-0798) or Tris/Tricine/SDS buffer (Bio-Rad, 161-0744) at 120V for 80min. Afterwards, the resolved proteins were transferred to polyvinylidene Difluoride (PVDF) membrane (Bio-Rad, 162-0177) at 100V for 60minutes. The blots were blocked with 5% skim milk in PBS-T for 60minutes with rocking and incubated overnight at 4°C with anti-6E10 specific antibody (1:1000, Biolegend, 803001), anti-Lamp1 specific antibody (1:1000, Abcam, ab24170), anti-LC3B specific antibody (1:2000, Sigma, L7543), anti- β -Actin specific antibody (1:2000, Sigma, A5441). After rinsed with PBS-T three times for 10minutes, the blots were further incubated with horseradish peroxidase-conjugated anti-mouse IgG (1:5000, Vector, PI-2000) or anti-rabbit IgG (1:5000, Vector, PI-1000) for 1-2hrs at room temperature and developed to film using ECL solution (Thermo, 34080 or Millipore, WBKLS0500). Band intensity of detected proteins were analyzed with ImageJ.

Immunocytochemistry

Microglial BV2 cells plated on PDL-coated and sterilized coverslips were washed with PBS two times and fixed with 4% PFA at 37°C for 15minutes. After rinsed with PBS three times for 5minutes, the cells were permeablized with 0.5% triton X-100 in PBS for 10minutes and quickly washed with PBS for 5minutes. The cultures were blocked for 1hour

with 10% normal goat serum, 0.1% tween-20, 5% BSA in PBS and incubated for overnight at 4°C with anti-6E10 specific antibody (1:100, Biolegend, 803001). Afterwards, the cells were washed with PBS three times for 10minutes and then incubated with anti-mouse-Alexa Fluor® 488 (1:200, Life technologies, A21202) at room temperature during 60minutes. For phalloidin staining, cultures were incubated with rhodamine phalloidin (1:40, Molecular probes, R-415) for 20min at room temperature. The cells were stained again with Hoeschst (1:1000, Sigma, H6204-10ML) for 10minutes at room temperature and washed with PBS three times for 5minutes. The coverslips were mounted onto glass slides using fluorescent mounting medium (DAKO, S3023). Fluorescence were detected with Nikon Eclipse Ti microscope and the image was processed with NIS-Elements microscope imaging software.

siRNA Transfection

The BV2 cells were transfected with 20nM of siC3AR1 and negative siRNA (siCTL) using lipofectamine 2000 (Invitrogen, 116688-019). siRNA and lipofectamine 2000 were respectively mixed with OptiMEM (Gibco, 31985-070) and incubated for 5minutes at room temperature. Afterwards, siRNA and lipofectamine were mixed again with gentle pipetting. After incubation for 25minutes at room temperature, the mixture was treated on cells. The media was changed after 4hrs with complete media and the cells were cultured at 5% CO₂ atmosphere for 48hours at 37°C. The sequences of used siRNA are as follows.

- C3AR1 siRNA = CTACCAGAAAGCAATTCTA

Real Time – quantitative PCR

Cultures were washed with PBS two times and incubated with 0.5mL TRIzol (Gibco, 15596-026) for 10minutes at room temperature to permit the complete dissociation of nucleoprotein complexes. After addition with 0.1mL chloroform (Sigma, C2342-500ML) with incubation at room temperature during for 10minutes, centrifuging was performed at 13,000rpm for 5minutes at 4°C and upper aqueous phase was collected. RNA was incubated with 0.25mL of isopropanol (Amresco, 0918-1L) at room temperature during 10minutes and centrifuged at 13,000rpm during 15minutes at 4°C. Then, RNA was treated with 1mL, 75% EtOH (Millipore, 64-17-5) and repeatedly centrifuged at 13,000rpm during 5minutes at 4°C.

The pellet of isolated RNA was dried with air for 10 minutes and dissolved with DEPC-treated water (Biosesang, W2004). The purified RNA stored at -80 °C until use. cDNAs was synthesized from 1 µg of the purified total RNA using Reverse transcription kit (Toyobo, FSQ101).

Real Time quantitative PCR was performed with Roche LightCycler 480 (Applied system) using iQ™ Sybr Green Supermix (Bio-Rad, 170-8880AP). Briefly, 20 ng of cDNAs was mixed with primers and performed with cycles as follows: 95 °C for 5 minutes, 45 cycles with 95 °C for 10 seconds, 60 °C for 10 seconds, 72 °C for 15 seconds, Melting Curve. The specific primers that used to determine mRNA levels are as follows and normalized to GAPDH.

- C3AR1 F = 5'-TCTCCTTGCCCTTCTCCTTG-3'
- C3AR1 R = 5'-TACCACCCAGACACATCCAC-3'
- TNF α F = 5'-GCCACCACGCTCTTCTGCCT-3'
- TNF α R = 5'-GGCTGATGGTGTGGGTGAGG-3'
- IL-6 F = 5'-CCGGAGAGGAGACTTCACAG-3'
- IL-6 R = 5'-TCCACGATTTCCCAGAGAAC-3'
- IL-1 β F = 5'-AAATACCTGTGGCCTTGGGC-3'
- IL-1 β R = 5'-CTTGGGATCCACACTCTCCAG-3'
- iNOS F = 5'-AATCTTGGAGCGAGTTGTGG-3'
- iNOS R = 5'-CAGGAAGTAGGTGAGGGCTTG-3'
- GAPDH F = 5'-GAACATCATCCCTGCATCCA-3'
- GAPDH R = 5'-CCAGTGAGCTTCCCGTTCA-3'

Results

TLQP-21 enhances microglial phagocytic activity.

Prior to the study of TLQP-21, experiments were required to determine whether TLQP-21 itself is toxic to cells. Therefore, BV2 microglial cells were treated with TLQP-21 (1 μ M) or vehicle for 24hours and then, cell cytotoxicity LDH assay and viability MTT assay were performed. The amounts of LDH released and of formazan produced by reduced MTT by mitochondrial dehydrogenases showed no differences on TLQP-21-treated group compared to vehicle-treated control group (Figure 2A and 2B). The peptide was not toxic to the cells, so they were used for further experiments.

To examine the microglial phagocytic activity, microglial BV2 cultures were treated with pre-opsonized latex beads and TLQP-21 (1 μ M) or LPS (10 μ g/ml) as positive control⁶⁷⁾ for 24hrs. Since latex beads are artificial materials that cannot be degraded by microglia, they are suitable for use in experiments to determine whether enhancing microglial phagocytosis. The phagocytic efficiency of latex beads was confirmed using immunocytochemistry and increased in TLQP-21 treated microglial BV2 cell lines compared to control group (Figure 3A). To get more accurate results, the latex beads engulfed microglial cells are counted with flow cytometry analysis. This data show increased number of latex bead-engulfed microglia in TLQP-21-treated cells compared to vehicle-treated control cells (Figure 3B). These data suggest that TLQP-21 improves the microglial phagocytic activity.

TLQP-21 increases fA β uptake on microglial BV2 cells.

In order to investigate the relationship between TLQP-21 and AD based on the effect of TLQP-21 promoting microglial phagocytic activity, BV2 microglial cells were treated with FITC-fibril A β (1 μ M) for increasing periods of time (30min, 1hr and 2hrs), after treated with TLQP-21 (1 μ M) for 30min. The flow cytometry analysis showed that intracellular A β levels were increased in TLQP-21 treated cells compared to control group (Figure 4A). To further confirm the effect of TLQP-21, TLQP-21 (1 μ M) was treated for 30min prior to treatment of fA β (1 μ M) for 2hrs on microglial BV2 cell lines and TLQP-21 increased intracellular A β levels (Figure 4B and 4C). These results suggest that TLQP-21 improves fA β uptake on

microglial cells.

C3AR1 is associated with TLQP-21-mediated A β uptake.

It was speculated that TLQP-21 might promote phagocytosis of microglial cells through activation of C3AR1 because TLQP-21 interacts with C3AR1, C3a complement receptor⁶²⁻⁶³. To verify the relationship between C3AR1 and TLQP-21-mediated microglial phagocytosis, I treated TLQP-21 (1 μ M) with or without SB290157 (10 μ M), C3AR1 antagonist, on microglial BV2 cells for 30minutes prior to treatment with fA β (1 μ M) for 2hours. The intracellular A β levels in the microglial cells treated with TLQP-21 were higher than those in the control group, whereas TLQP-21 and SB290157 co-treated microglial cells showed a decrease in intracellular A β levels than TLQP-21-treated cells (Figure 5A and 5B).

To further confirm whether TLQP-21-mediated fA β phagocytosis can be blocked by C3AR1 inhibition, siC3AR1 and negative siRNA were transfected for 48hours using lipofectamine and then treated with TLQP-21 (1 μ M) and fA β (1 μ M) on microglial BV2 cells. Decreased mRNA level of C3AR1 by transfection with siC3AR1 was confirmed using RT-quantitative PCR (Figure 6A) and knockdown of C3AR1, in line with previous data, decreased A β protein level despite the treatment of TLQP-21 (Figure 6B and 6C). These results suggest that inhibition of C3AR1 attenuates TLQP-21-mediated microglial fA β phagocytosis.

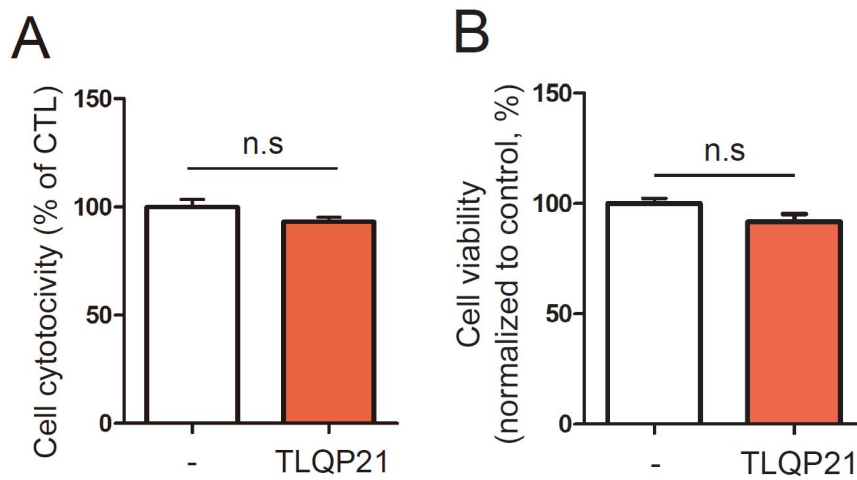


Figure 2. TLQP-21 has no toxicity to microglial BV2 cells.

TLQP-21 (1 μ M) was treated on microglial BV2 cells for 24hrs to evaluate the effect of TLQP-21 on cell cytotoxicity and the amount of LDH release was analyzed using cell cytotoxicity LDH kit (A). Microglial BV2 cells were also treated with TLQP-21 (1 μ M) and fA β (1 μ M) for 24hrs and cell death was analyzed with MTT assay (B).

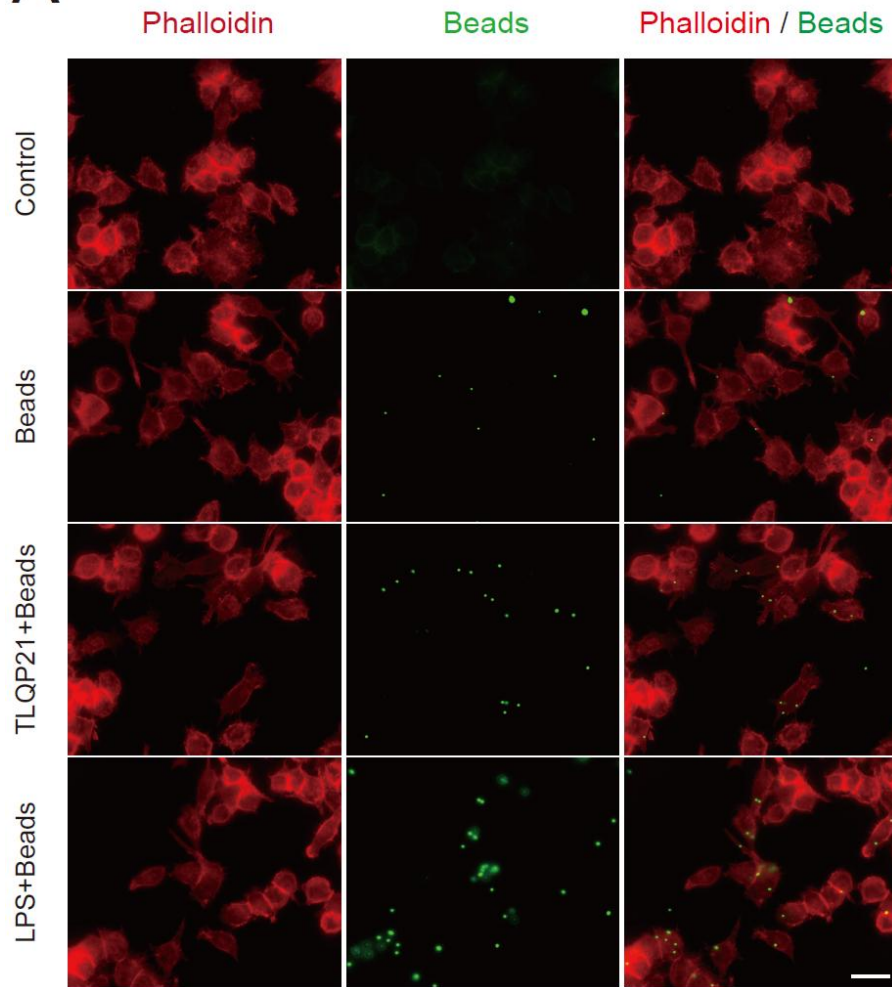
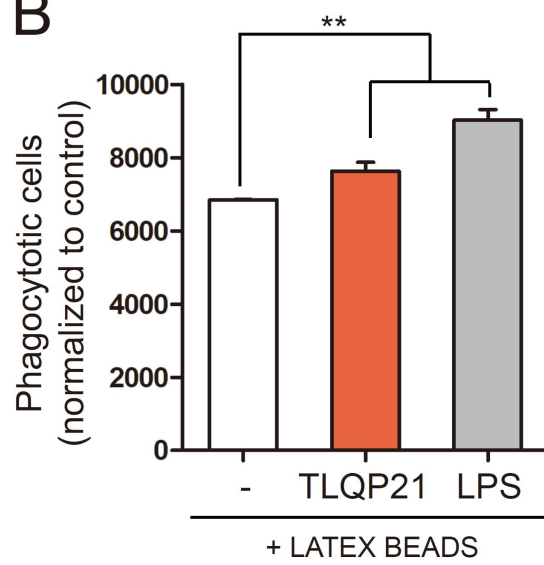
A**B**

Figure 3. TLQP-21 induces microglial phagocytosis without fA β .

BV2 microglial cells were treated with FITC-labeled and pre-opsionized latex beads with or without TLQP21 (1 μ M) for investigating the effects of TLQP-21 on phagocytic ability without fA β and immunocytochemistry was performed with anti-Iba1 antibody (A). Scale bar = 20 μ m. Microglial BV2 cells were treated with TLQP-21 (1 μ M) or LPS (10 μ g/ml) and the graph of flow cytometry shows the number of phagocytic cells fed artificial substrates (B). Student t-test was used for statistical analysis (**p<0.01).

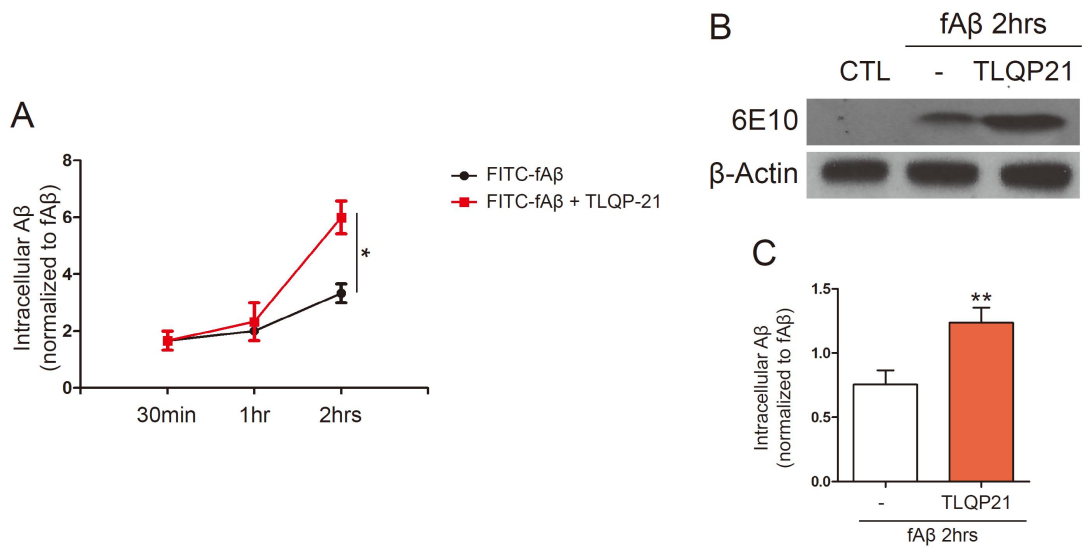


Figure 4. TLQP-21 increases intracellular A β protein level on microglial BV2 cells.

Microglial BV2 cells were treated with TLQP-21 (1 μ M) or vehicle for 30min prior to fA β (1 μ M) treatment for 2hrs. For the quantification of intracellular A β proteins, immunoblots were performed with anti-6E10 and anti-Phospho-P38 specific antibody (A) and β -actin, p38 were used as control (B and C). Statistical analysis was performed using student t-test. (* p <0.05, ** p <0.01, *** p <0.001).

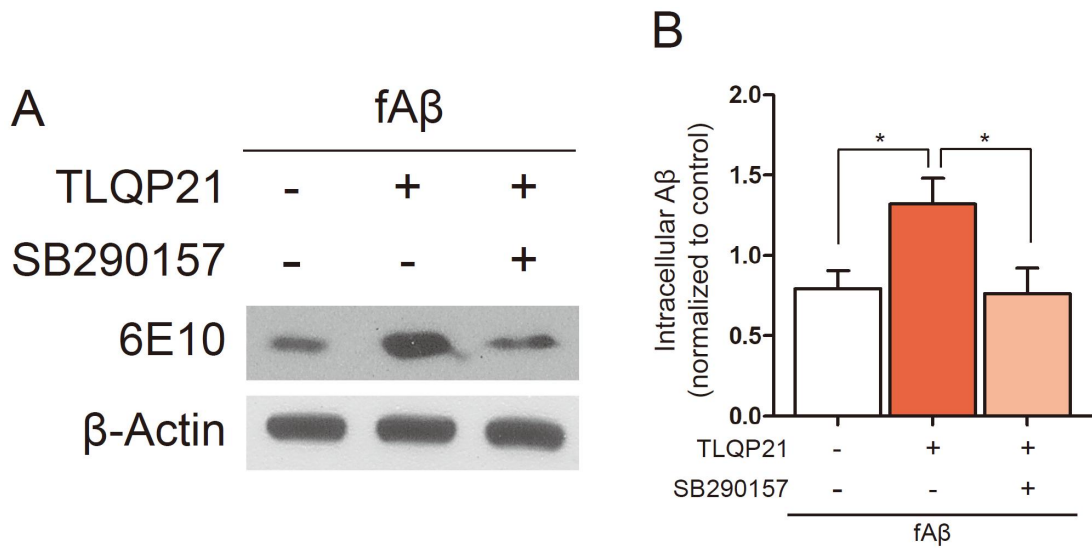


Figure 5. C3AR1 treatment antagonist attenuates TLQP-21-mediated microglial fA β phagocytosis

Before treatment with fA β (1 μ M) during 2hrs, microglial BV2 cells were pre-treated with or without TLQP21 (1 μ M) and SB290157, C3AR1 antagonist, (10 μ M) during 30min. Cultures were analyzed by immunoblot with anti-6E10 (A) and β -actin was used as normalized control (B). Statistical analysis was performed with student t-test. (* p <0.05).

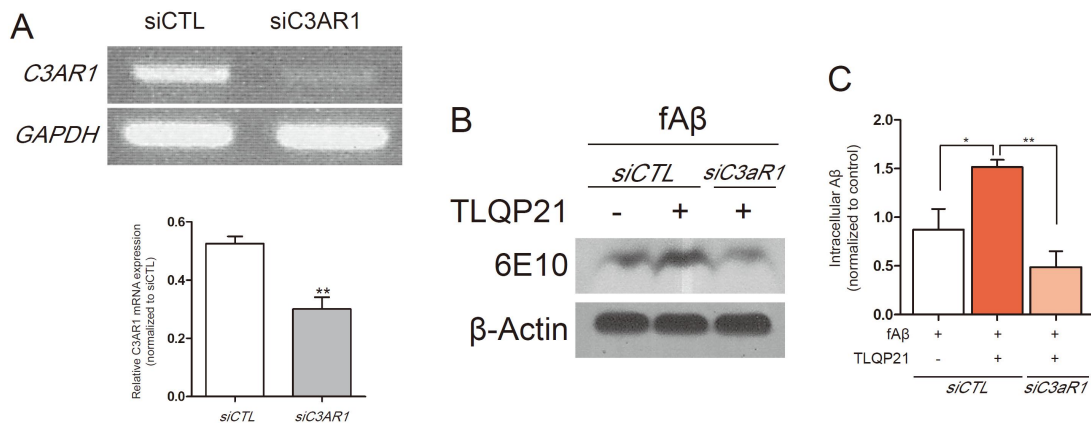


Figure 6. siC3AR1 transfection attenuates TLQP-21-mediated microglial fAβ phagocytosis

BV2 microglial cells transfected with siC3AR1 or siCTL for 48hrs were treated with fAβ (1μM, 2hrs) and TLQP-21 (1μM, 30min) or only fAβ (1μM, 2hrs). Efficiency of transfection with siC3AR1 was demonstrated using RT-qPCR and it was normalized with GAPDH (A). Immunoblot was performed with anti-6E10 (B) and the data was normalized with β-actin (C). Statistical values was tested using student t-test. (*p<0.05, **p<0.01).

TLQP-21 improves microglial A β clearance.

If microglial cells cannot effectively degrade the toxic proteins or apoptotic cells they uptake, the substances will accumulate in the brain environment and deteriorate neurodegeneration, even if microglial cells engulf them. As such, the clearance of toxic proteins by microglia is another important mechanism for delaying neurodegenerative disorders. Thus, TLQP-21-treated cells were treated with fA β (1 μ M) for 2hrs (T0, 0hrs after removal of fA β) and then conditioned medium were placed with fresh medium without fA β . Thereafter the cells were incubated for 3hrs (T3, 3hrs after removal of fA β) and 6hrs (T6, 6hrs after removal of fA β), in order to observe the effect of degradation under the environment where the A β uptake is excluded (Figure 7A). This data demonstrates that intracellular A β levels of TLQP-21-treated cells were increased in T0 time point, but surprisingly reduced after the removing of fA β (T3 and T6 time points) compared to the control group (Figure 7B).

For visualization of TLQP-21-mediated microglial fA β uptake and degradation, TLQP-21 and fA β - treated BV2 cells stained with an anti-6E10 antibody on indicated time point. As a result, the amount of intracellular A β in TLQP-21-treated cells was increased in T0 time point and decreased in T6 time point, as in the previous data (Figure 8). These results suggest that TLQP-21 enhances microglial A β clearance by promoting A β phagocytosis and degradation.

TLQP-21 degrades engulfed A β via stimulation of lysosomal degradation pathway.

To determine whether TLQP-21 degrades A β via lysosomal or proteasomal degradation pathway, TLQP-21-treated microglial BV2 cultures were treated with fA β (1 μ M) and Baf.A1 (100nM) or MG132 (5 μ M). The medium of these cells was changed to new medium without fA β and incubated in the same way as Figure 7 to determine the mechanism of A β degradation. In the MG132 treatment, intracellular A β levels were decreased in time-dependent manner similar to TLQP-21 treated control cells (Figure 9A and 9C). But interestingly, intracellular A β levels in Baf.A1 treated cells were retained. (Figure 9A and 9B). These results indicate that TLQP-21 enhances A β clearance via modulating of lysosomal degradation pathway.

In order to confirm whether TLQP-21 stimulates lysosomal function or autophagy, the markers of each mechanism on TLQP-21-treated cultures are observed by western blot. First, protein levels of Lamp1 were observed and increased in TLQP-21-treated cells compared to only fA β -treated cells (Figure 10A and 10B). Since Lamp1 is a lysosomal membrane protein, this data suggest that TLQP-21 promotes the formation of lysosomes. Next, quantitative changes of LC3B-II on TLQP-21-treated cells were observed, because it is an autophagy marker capable of autophagosome biogenesis. TLQP-21 increased LC3B-II protein levels at T0 time point compared to fA β and the increased LC3B-II was eliminated more rapidly than the control group (Figure 10A and 10C). These results implies that TLQP-21 enhances the fusion of autophagosome and lysosome.

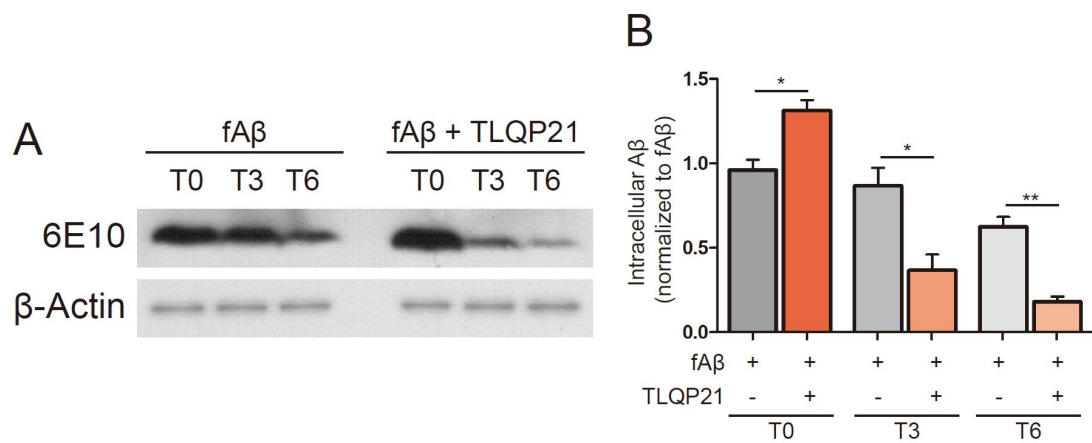


Figure 7. TLQP-21 promotes microglial A β degradation.

Microglial BV2 cell lines were treated with fA β (1 μ M) for 2hrs after TLQP-21 (1 μ M) treatment for 30min (T0). After changing to fresh medium without fA β , BV2 cell lines were cultured during 3hrs (T3) and 6hrs (T6). Intracellular A β levels were analyzed using immunoblot (A) and the graph showed quantification of western blot data (B). Student t-test was used for analyzing statistical values (* <0.05 , ** <0.01).

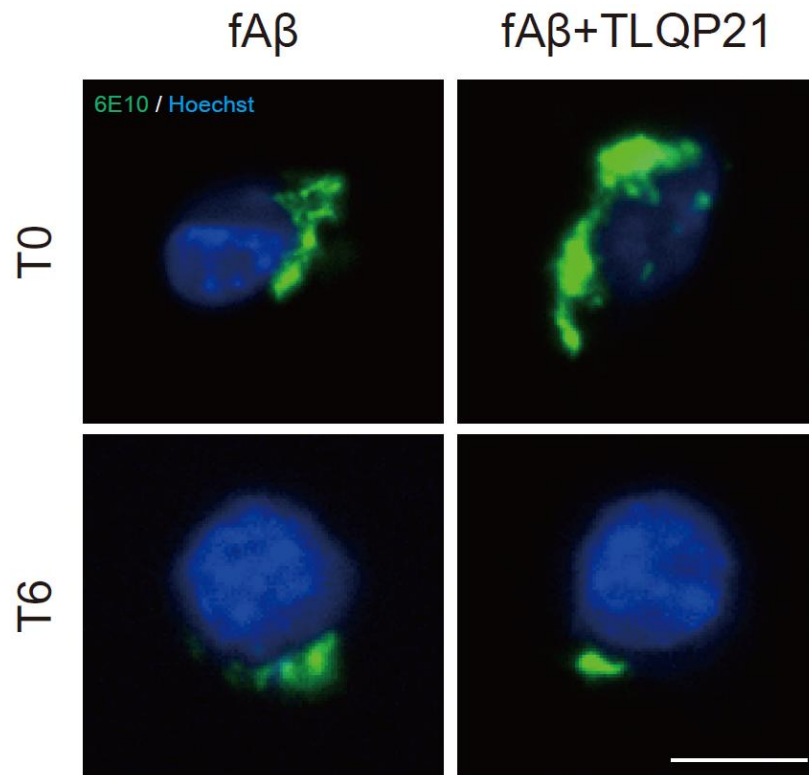


Figure 8. TLQP-21-treated microglial BV2 cultures more degrades engulfed A β .

BV2 cells were treated with fA β (1 μ M) for 2hrs after TLQP-21 (1 μ M) treatment for 30min (T0). After changing to fresh medium without fA β , the cells were incubated during 6hrs (T6). A β internalization (T0) and degradation (T6) were detected with immunocytochemistry using anti-6E10. Scale bar = 20 μ m.

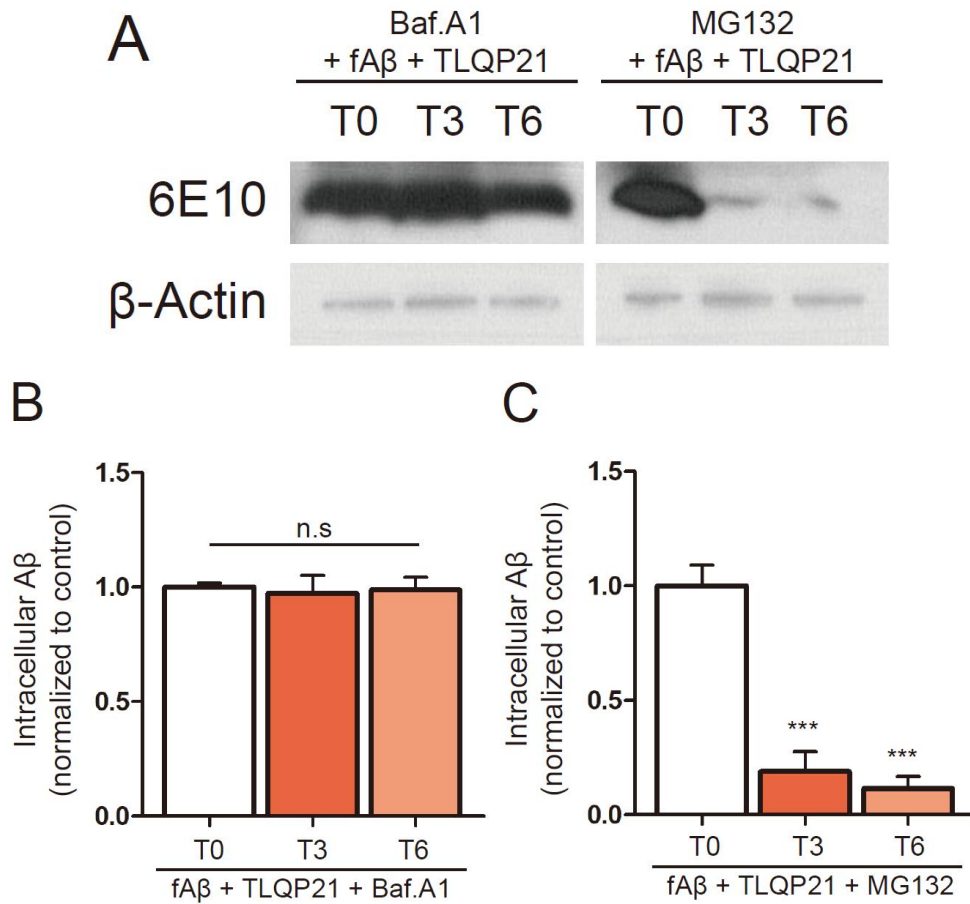


Figure 9. Lysosomal degradation pathway is related to TLQP-21-mediated microglial A β degradation

Microglial BV2 cell lines were treated with fA β (1 μ M) for 2hrs after TLQP-21 (1 μ M) treatment for 30min (T0). After changing to fresh medium without fA β , BV2 cell lines were cultured during 3hrs (T3) and 6hrs (T6). Intracellular A β levels were analyzed using immunoblot (A) and the quantification data of Baf.A1 or MG132-treated cultures were represented graphically (B and C). Statistical values were calculated with student t-test (^{n.s.}p>0.05, ^{***}p<0.001).

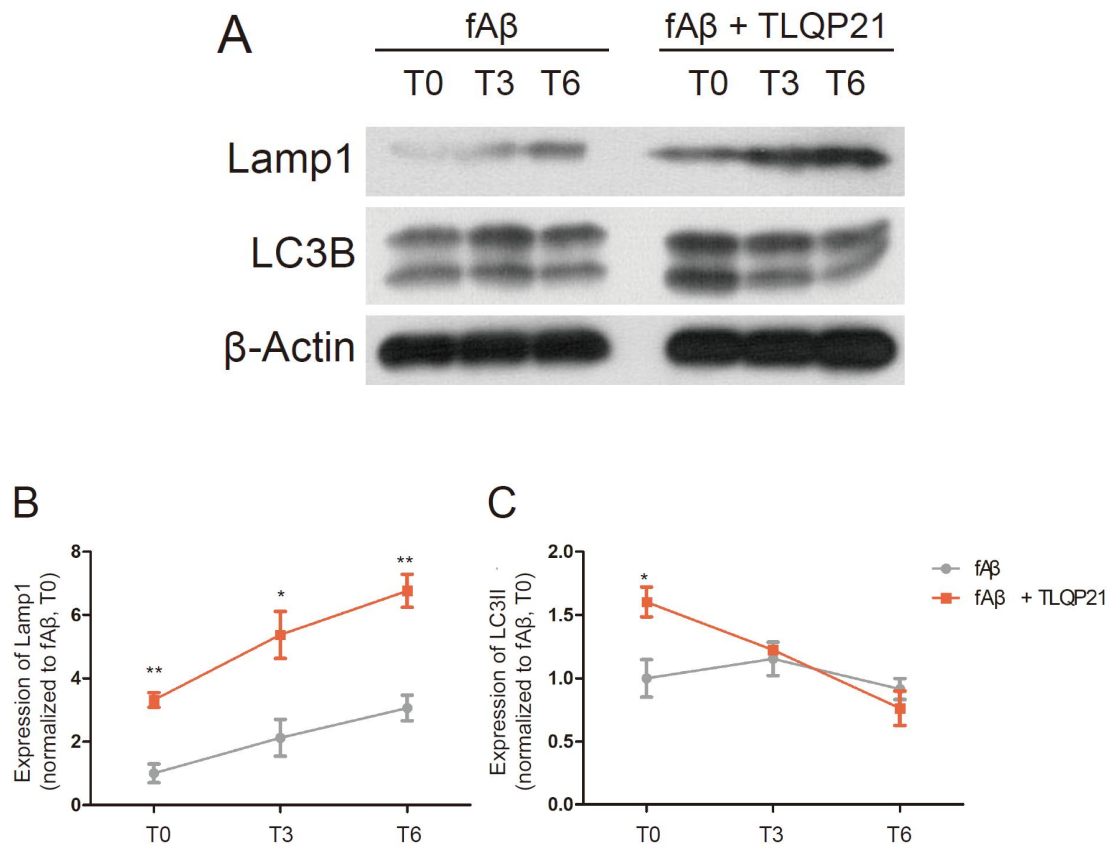


Figure 10. TLQP-21 stimulates lysosomal degradation pathway.

TLQP-21 or vehicle -treated microglial BV2 cells were treated with fA β for 2hrs. After changing medium, cultures were incubated 3hrs and 6hrs. Immunoblot was performed to analyze protein levels of Lamp1 and LC3B (A). The graphs indicated the quantification data (B and C). Student t-test was used to calculate statistical values (* $p < 0.05$, ** $p < 0.01$).

TLQP-21 has no effect on inflammation-related cytokines release.

Microglia play dual role as A β uptake and releasing cytotoxic inflammatory cytokines and these released cytokines has neurotoxicity⁶⁸. To investigate whether TLQP-21 stimulates release of inflammatory cytokine on microglia, LPS (10 μ g/ml) with or without TLQP-21 (1 μ M) were treated on microglial BV2 cells during 24hours and analyzed Real Time-quantitative PCR with inflammation-related cytokines such as TNF α , IL-1 β , IL-6 and iNOS and GAPDH was used as normalization control. The mRNA levels of TNF α were decreased when compared to LPS-treated cells, but the intensity of decrease is not statistically enough and the mRNA levels of other cytokines were not modulated in TLQP-21-treated microglial cells (Figure 10A – 10D). These data suggest that TLQP-21 does not cause negative effect on microglial inflammation.

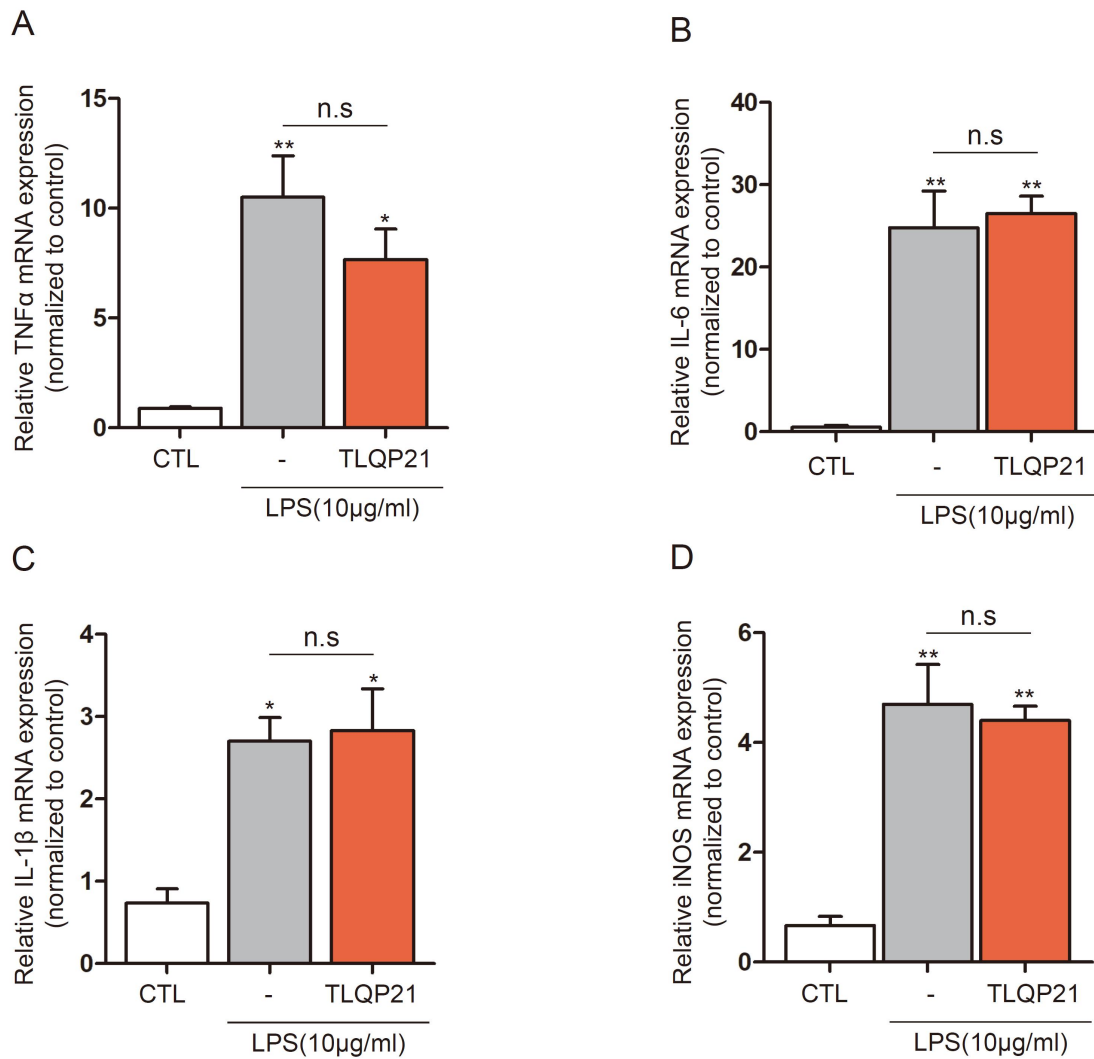


Figure 11. TLQP-21 shows no change on release of inflammation-related cytokines.

Microglial BV2 cells were treated with LPS (10μg/ml) for 24hrs with or without pre-treatment of TLQP-21 (1μM) for 30min. Real Time – quantitative PCR was performed with TNFα (A), IL-6 (B), iNOS (C) and IL-1β (D) and the analysis was normalized to GAPDH. Statistical values was tested with student t-test. (*p<0.05, **p<0.01).

Discussion

In this study, I first demonstrated that TLQP-21 enhances clearance of extracellular fibril A β by BV2 microglial cells. TLQP-21, the bioactive peptides derived from the C-terminal of VGF precursor protein, improves microglial phagocytic activity and fibril A β uptake by microglia. C3AR1 is related with TLQP-21-mediated A β phagocytosis. TLQP-21 also promotes degradation of engulfed A β by microglia and TLQP-21 increased the markers of autophagy, Lamp1 and LC3B-II.

The reduction of VGF-derived peptides in CSF of AD patients has already been reported⁶⁴⁾ and this quantitative change of these peptides implies the association of the pathogenesis of AD with the quantitative modulation of VGF-derived peptides. Thus, there is a possibility that various VGF-derived peptides may influence the pathogenesis of AD in various ways. In addition, several reports indicate that TQLP-21 can modulate microglial function⁶⁵⁾ and, in fact, TLQP-21 improves the phagocytic activity of microglial BV2 cell cultures in bead-based phagocytosis assay (Figure 3). Based on this result, it is considered whether TLQP-21 affects AD pathology by modulating in phagocytosis of A β , which is the major pathologic factor of AD and TLQP-21 also promotes phagocytosis of fibril A β (Figure 4). The stimulation of A β phagocytic activity by microglial cells is thought to be the result of the increase of phagocytic activity. This result imply that TLQP-21 promotes fA β uptake only through phagocytosis, micropinocytosis and endocytosis.

Complement C3 plays several roles as mediators of innate immunity⁶⁹⁻⁷⁰⁾ and microglial engulfment in CNS and is known to be involved in target recognition, migration and phagocytosis of microglia⁷¹⁻⁷²⁾. C3a is produced by cleavage of C3, binds to C3AR1 as a ligand. It has been reported that treatment of the complement on microglial cells for a short period of time promotes A β phagocytosis⁶⁶⁾. On the same line, my data showed that TLQP-21 also promotes microglial phagocytosis of fA β and pre-opsonized latex beads (Figure 3 and 4). This suggests that C3AR1 exerts an influence on fA β phagocytosis.

Among VGF-derived peptides, TLQP-21 is known peptide whose receptor on microglia

or macrophage has been identified and C3AR1, C3a complement protein receptor 1, is known as one of its receptors⁶²⁻⁶³). Furthermore, the function of TLQP-21 on microglial A β phagocytosis was suppressed when C3AR1 was blocked using C3AR1 antagonist or transfection with siC3AR1 (Figure 10 and 11). This indicates that the interaction with C3AR1 is a necessary process for promoting microglial action of TLQP-21 on microglia.

TLQP-21 enhances A β degradation and this clearance effect is mediated to lysosomal degradation pathway (Figure 7 – 10). TLQP-21-mediated A β degradation is inhibited by treatment of Baf.A1 but not MG132 (Figure 9). MG132 blocks the proteolytic activity of proteasome complex as a proteasome inhibitor⁷³) and Baf.A1 known to inhibit later stages of autophagy inhibits the activity of vacuolar-type H (+)-ATPase, thereby blocking the acidification of lysosome⁷⁴). Baf.A1 is also known to block the fusion of autophagosome and lysosome⁷⁵). Therefore, the mechanism of TLQP-21-mediated A β degradation is promoted by controlling the activity of lysosome rather than that of proteasome.

Several attempts have been made to remove amyloid plaques and it has recently been shown that autophagy play an important role in microglial A β clearance⁷⁶). Autophagy is a destructive mechanism that naturally breaks down unnecessary or nonfunctional cellular constituents during regulation⁷⁷). Misfolded or unwanted proteins are ubiquitinated and bind to adaptor proteins when the protein are exposed in intracellular space and LC3II interacts with the polyubiquitinated protein-adaptor protein complex as a component of autophagosome⁷⁸⁻⁷⁹). This autophagosome is fused with the lysosome to form an autolysosome, which degrades the proteins. When autophagy is activated, LC3II is increased within a short time, but autolysosome is gradually formed and functions and LC3II is also reduced naturally⁸⁰). In my result, LC3II was increased in TLQP-21 treated cells compared to control, and the rate of elimination was also rapid (Figure 10), suggesting that TLQP-21 promotes autophagosome formation and fusion with lysosomes. Additionally, TLQP-21 increased the protein levels of Lamp1 (Figure 10). This indicates that TLQP-21 enhances the formation of lysosome. In all of these results, therefore, it is believed that TLQP-21 enhances the efficiency of A β degradation by promoting the function of autophagosome and lysosomes. The induction of autophagy occurs via pathway mediated by AMPK or PI3KC3

and stimulation through these paths induces autophagy by modulating mTOR or ULK1⁸¹⁻⁸²). It is assumed that TLQP-21 induces autophagy through the corresponding signaling (Data not shown).

A β clearance of TLQP-21-treated microglia can lead to neuroprotective effects in terms of physically eliminating A β . However, A β -stimulated microglia can release various cytokines associated with inflammation through signaling by interacting with A β , which leads to toxicity on neuronal cells^{39, 68}). Interestingly, TLQP-21 did not affect the release of inflammation-related cytokines (Figure 11). In particular, although the change was not significant, TLQP-21 was observed to decrease the mRNA levels of TNF α . These findings demonstrate that TLQP-21 promotes the microglial A β phagocytosis without inflammation and may possibly lead to an anti-inflammatory effect by reducing the expression of TNF α . All data suggest that TLQP-21 was found to induce clearance of fA β without affecting inflammation, further suggesting that TLQP-21 may have a neuroprotective effects by physically promoting microglial A β clearance in the brain environment.

In summary, TLQP-21 increases intracellular A β levels through C3AR1-dependent mechanism and also improves microglial A β degradation via enhancement of lysosomal function and the induction of autophagy on microglial BV2 cell lines, shown as Figure 12. In addition, TLQP-21 doesn't affect the induction of inflammation by microglial activation or microglial A β clearance. Since TLQP-21 promotes the A β clearance of microglia without inducing inflammation, therefore, I suggest that TLQP-21 may have protective effects on neurons and may be developed as a new therapeutic agent for AD.

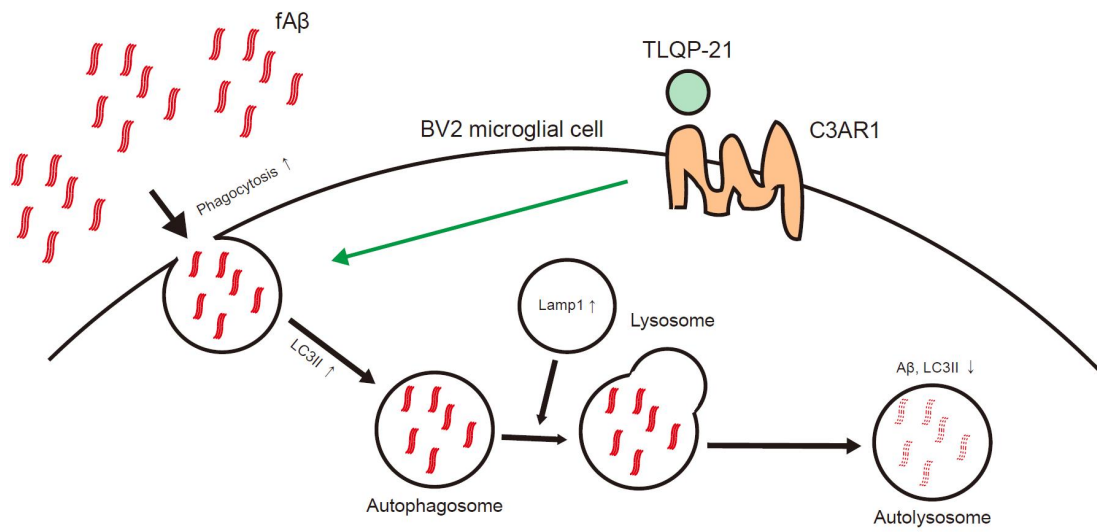


Figure 12. Proposed model of TLQP-21 functions in the microglial Aβ clearance.

In microglial BV2 cells, TLQP-21 stimulates phagocytosis and fAβ uptake and this uptake is C3AR1-dependent mechanism. TLQP-21 also promotes engulfed Aβ degradation through enhancement of the lysosomal degradation pathway.

References

1. Burns A, Iliffe S. Alzheimer's disease. *BMJ* 2009; 338:b158.
2. DeKosky ST, Scheff SW. Synapse loss in frontal cortex biopsies in Alzheimer's disease. *Ann Neurol* 1990; 27(5):457-64.
3. Terry RD, Masliah E, Salmon DP, Butters N, De Teresa R, Hill R, et al. Physical basis of cognitive alterations in Alzheimer's disease: synapse loss is the major correlate of cognitive impairment. *Ann Neurol* 1991; 30(4):572-80.
4. Arendt T. Synaptic degeneration in Alzheimer's disease. *Acta Neuropathol* 2009; 118(1):167-79.
5. Berchtold NC, Cotman CW. Evolution in the conceptualization of dementia and Alzheimer's disease : Greco-roman period to the 1960s. *Neurobiol Aging* 1998; 19(3):173-89
6. Mendez MF. Early-onset Alzheimer's disease: nonamnestic subtypes and Type 2 AD. *Arch Med Res* 2012; 43(8): 677-85.
7. Hebert LE, Scherr PA, Bienias JL, Bennett DA, Evans DA. Alzheimer's disease in the US population: prevalence estimates using the 2000 census. *Arch Neurol* 2003; 60(8): 1119-22.
8. Brookmeyer R, Johnson E, Zeigler-Graham K, Arrighi HM. Forecasting the global burden of Alzheimer's disease. *Alzheimer's Dement* 2007; 3(3): 186-91.
9. Tilley L, Morgan K, Kalsheker N. Genetic risk factors in Alzheimer's disease. *Mol Pathol* 1998; 51(6): 293-304.
10. Scheuner D, Eckman C, Jensen M, Song X, Citron M, Suzuki N, et al. Secreted amyloid beta-protein similar to that in the senile plaques of Alzheimer's disease is increased in vivo by the presenilin 1 and 2 and APP mutations linked to familial Alzheimer's disease. *Nat Med* 1996; 2(8):864-70.
11. Levy-Lahad, E. et al. Candidate gene for the chromosome 1 familial Alzheimer's disease locus. *Science* 1995; 269:973-977.
12. Corder, E. H. et al. Gene dose of apolipoprotein E type 4 allele and the risk of Alzheimer's disease in late onset families. *Science* 1993; 261:921-923.
13. Chartier-Harlin, M. C. et al. Apolipoprotein E, epsilon 4 allele as a major risk factor for

- sporadic early and late-onset forms of Alzheimer's disease: Analysis of the 19q13.2 chromosomal region. *Hum Mol Genet* 1994; 3:569-574.
14. Yoon SY, Kim DH. Alzheimer's disease genes and autophagy. *Brain Res* 2016; 1649(Pt B): 201-209.
 15. Wilcock GK, Esiri MM. Plaques, tangles and dementia. A quantitative study. *J Neurol Sci* 1982; 56(2-3): 343-56.
 16. Hardy J, Selkoe DJ. The amyloid hypothesis of Alzheimer's disease: progress and problems on the road to therapeutics. *Science* 2002; 297(5580):353-6.
 17. Ballatore C, Lee VM, Trojanowski JQ. Tau-mediated neurodegeneration in Alzheimer's disease and related disorders. *Nat Rev Neurosci* 2007; 8(9): 663-72.
 18. Iqbal K, Alonso Adel C, Chen S, Chohan MO, El-Akkad E, Gong CX, et al. Tau pathology in Alzheimer disease and other tauopathies. *Biochim Biophys Acta* 2005; 1739(2-3): 198-210
 19. Morishima-Kawashima M, Hasegawa M, Takio K, Suzuki M, Yoshida H, Watanabe A, et al. Hyperphosphorylation of Tau in PHF. *Neurobiol Aging* 1995; 16(3): 365-71.
 20. Zhang YW, Thompson R, Zhang H, Xu H. APP processing in Alzheimer's disease. *Mol Brain* 2011; 4: 3.
 21. Zheng H, Koo EH. The amyloid precursor protein: beyond amyloid. *Mol Neurodegener* 2006; 1: 5.
 22. Allinquant B, Hantraye P, Mailleux P, Moya K, Bouillot C, Prochiantz A. Downregulation of amyloid precursor protein inhibits neurite outgrowth in vitro. *J Cell Biol* 1995; 128(5): 919-27.
 23. Moya KL, Benowitz LI, Schneider GE, Allinquant B. The amyloid precursor protein is developmentally regulated and correlated with synaptogenesis. *Dev Biol* 1994. 161(2): 597-603.
 24. Gunawardena S, Goldstein LS. Disruption of axonal transport and neuronal viability by amyloid precursor protein mutations in drosophila. *Neuron* 2001; 32(3): 389-401.
 25. Koo EH, Sisodia SS, Archer DR, Martin LJ, Weidemann A, Beyreuther K, et al. Precursor of amyloid protein in Alzheimer's disease undergoes fast anterograde axonal transport. *Proc Natl Acad Sci USA* 1990; 87(4): 1651-5.

26. Yamazaki T, Selkoe DJ, Koo EH. Trafficking of cell surface amyloid-precursor protein: retrograde and transcytotic transport in cultured neurons. *J Cell Biol* 1995; 129(2): 431-42.
27. Lyckman AW, Confaloni AM, Thinakaran G, Sisodia SS, Moya KL. Post-translational processing and turnover kinetics of presynaptically targeted amyloid precursor superfamily proteins in the central nervous system. *J Biol Chem* 1998; 273(18): 11100-6.
28. Vassar R, Bennett BD, Babu-Khan S, Kahn S, Mendiaz EA, Denis P, et al. Beta-secretase cleavage of Alzheimer's amyloid precursor protein by the transmembrane aspartic protease BACE. *Science* 1999; 286(5440):735-41.
29. McLean CA, Cherny RA, Fraser FW, Fuller SJ, Smith MJ, Beyreuther K, et al. Soluble pool of abeta amyloid as a determinant of severity of neurodegeneration in Alzheimer's disease. *Ann Neurol* 1999; 46(6): 860-6.
30. Tu S, Okamoto S, Lipton SA, Xu H. Oligomeric A β -induced synaptic dysfunction in Alzheimer's disease. *Mol Neurodegener* 2014; 9: 48.
31. Chen JX, Yan SD. Amyloid-beta induced mitochondrial dysfunction. *J Alzheimers Dis* 2007; 12(2): 177-84.
32. Tai LM, Ghura S, Koster KP, Liakaite V, Maienschein-Cline M, Kanabar P, et al. APOE-modulated A β -induced neuroinflammation in Alzheimer's disease: current landscape, novel data and future perspective. *J Neurochem* 2015; 133(4): 465-88.
33. Takagane K, Nojima J, Mitsuhashi H, Suo S, Yanagihara D, Takaiwa F, et al. A β induces oxidative stress in senescence-accelerated (smp8) mice. *Biosci Biotechnol Biochem* 2015; 79(6): 912-8.
34. Gehrman J, Matsumoto Y, Kreutzberg GW. Microglia: Intrinsic immune effector cell of the brain. *Brain Res Brain Res Rev* 1995; 20(3): 269-87.
35. Paresce DM, Ghosh RN, Maxfield FR. Microglial cells internalize aggregates of the AD amyloid beta-protein via a scavenger receptor. *Neuron* 1996; 17(3): 553-65.
36. Koenigsknecht J, Landreth G. Microglial phagocytosis of fibrillar beta-amyloid through beta1 integrin-dependent mechanism. *J Neurosci* 2004; 24(44): 9838-46.
37. Mandrekar S, Jiang Q, Lee CY, Koenigsknecht-Talboo J, Holtzman DM, Landreth GE. Microglia mediate the clearance of Soluble Abeta through fluid phase micropinocytosis.

- J Neurosci 2009; 29(13): 4252-62.
38. Mohamed A, Posse de Chaves E. A β Internalization by Neurons and Glia. *Int J Alzheimers Dis* 2011; 2011: 127984.
 39. Mosher KI, Wyss-Coray T. Microglial dysfunction in brain aging and Alzheimer's disease. *Biochem Pharmacol* 2014; 88(4): 594-604.
 40. Levi A, Eldridge JD, Paterson BM. Molecular cloning of a gene sequence regulated by nerve growth factor. *Science* 1985; 229(4711): 393-5.
 41. van den Pol AN, Bina K, Decavel C, Ghosh P. VGF expression in the brain. *J Comp Neurol* 1994; 347(3): 455-69.
 42. Lombardo A, Rabacchi SA, Cremini F, Pizzorusso T, Cenni MC, Possenti R, et al. A developmentally regulated nerve growth factor-induced gene, VGF, is expressed in geniculocortical afferents during synaptogenesis. *Neuroscience* 1995; 65(4): 997-1008.
 43. Synder SE, Salton SR. Expression of VGF mRNA in the adult rat central nervous system. *J Comp Neurol* 1998; 394(1): 91-105.
 44. Hahm S, Mizuno TM, Wu TJ, Wisor JP, Priest CA, Kozak CA, et al. Targeted deletion of the VGF gene indicates that the encoded secretory peptide precursor plays a novel role in the regulation of energy balance. *Neuron* 1999; 23(3): 537-48.
 45. Synder SE, Peng B. Expression of VGF mRNA in developing neuroendocrine and endocrine tissues. *J Endocrinol* 2003; 179(2): 227-35.
 46. Trani E, Giorgi A, Canu N, Amadoro G, Rinaldi AM, Halban PA, et al. Isolation and characterization of VGF peptides in rat brain. Role of PC1/3 and PC2 in the maturation of VGF precursor. *J Neurochem* 2002; 81(3): 565-74.
 47. Levi A, Ferri GL, Watson E, Possenti R, Salton SR. Processing, distribution, and function of VGF, a neuronal endocrine peptide precursor. *Cell Mol Neurobiol* 2004; 24(4): 517-33.
 48. Fujihara H, Sasaki K, Mishiro-Sato E, Ohbuchi T, Dayanithi G, Yamasaki M, et al. Molecular characterization and biological function of neuroendocrine regulatory peptide-3 in the rat. *Endocrinology* 2012; 153(3): 1377-86.
 49. D'Amato F, Noli B, Angioni L, Cossu E, Incani M, Messana I, et al. VGF peptide profiles in type 2 diabetic patients' plasma and in obese mice. *PLoS One* 2015; 10(11):

e0142333.

50. Toshinai K, Nakazato M. Neuroendocrine regulatory peptide -1 and -2: novel bioactive peptides processed from VGF. *Cell Mol Life Sci* 2009; 66(11-12): 1939-45.
51. Thakker-Varia S, Krol JJ, Nettleton J, Bilimoria PM, Bangasser DA, Shors TJ, et al. The neuropeptide VGF produces antidepressant-like behavioral effects and enhances proliferation in the hippocampus. *J Neurosci* 2007; 27(45): 12156-67.
52. Thakker-Varia S, Behnke J, Doobin D, Dalal V, Thakkar K, Khadim F, et al. VGF (TLQP-62)-induced neurogenesis targets early phase neural progenitor cells in the adult hippocampus and requires glutamate and BDNF signaling. *Stem Cell Res* 2014; 12(3): 767-77.
53. Bozdagi O, Rich E, Tronel S, Sadahiro M, Patterson K, Shapiro ML, et al. The neurotrophin-inducible gene VGF regulates hippocampal function and behavior through a brain-derived neurotrophic factor-dependent mechanism. *J Neurosci* 2008; 28(39): 9857-69.
54. Lin WJ, Jiang C, Sadahiro M, Bozdagi O, Vulchanova L, Alberini CM, et al. VGF and its C-terminal peptide TLQP-62 regulate memory formation in hippocampus via a BDNF-TRKB-dependent mechanism. *J Neurosci* 2015; 35(28): 10343-56.
55. Alder J, Thakker-Varia S, Bangasser DA, Kuroiwa M, Plummer MR, Shors TJ, et al. Brain-derived neurotrophic factor-induced gene expression reveals novel actions of VGF in hippocampal synaptic plasticity. *J Neurosci* 2003; 23(34): 10800-8.
56. Succu S, Cocco C, Mascia MS, Melis T, Melis MR, Possenti R, et al. Pro-VGF-derived peptides induce penile erection in male rats: possible involvement of oxytocin. *Eur J Neurosci* 2004; 20(11): 3035-40.
57. Lewis JE, Brameld JM, Hill P, Cocco C, Noli B, Ferri GL, et al. Hypothalamic over-expression of VGF in the Siberian hamster increases energy expenditure and reduces body weight gain. *PLoS One* 2017; 12(2): e0172724.
58. Jiang C, Lin WJ, Sadahiro M, Shin AC, Buettner C, Salton SR. Embryonic ablation of neuronal VGF increases energy expenditure and reduces body weight. *Neuropeptides* 2016; 64: 75-83.
59. Bartolomucci A, La Corte G, Possenti R, Locateli V, Rigamonti AE, Torsello A, et al.

- TLQP-21, a VGF-derived peptides, increases energy expenditure and prevents the early phase of diet-induced obesity. *Proc Natl Acad Sci USA* 2006; 103(39): 14584-9.
60. Cero C, Razzoli M, Han R, Sahu BS, Patricelli J, Guo Z, et al. The neuropeptide TLQP-21 opposes obesity via C3AR1-mediated enhancement of adrenergic-induced lipolysis. *Mol Metab* 2017; 6(1): 148-158.
61. Chen YC, Pristerá A, Ayub M, Swanwick RS, Karu K, Hamada Y, et al. Identification of a receptor for neuropeptide VGF and its role in neuropathic pain. *J Biol Chem* 2013; 288(48): 34638-46.
62. Hannedouche S, Beck V, Leighton-Davies J, Beibel M, Roma G, Oakeley EJ, et al. Identification of the C3a receptor (C3AR1) as the target of the VGF-derived peptide TLQP-21 in rodent cells. *J Biol Chem* 2013; 288(38): 27434-43.
63. Cero C, Vostrikov VV, Veradi R, Severini C, Gopinath T, Braun PD, et al. The TLQP-21 peptide activates the G-protein-coupled receptor C3AR1 via a folding-upon-binding mechanism. *Structure* 2014; 22(12): 1744-1753.
64. Cocco C, D'Amato F, Noli B, Ledda A, Brancia C, Bongioanni P, et al. Distribution of VGF peptides in the human cortex and their selective changes in Parkinson's and Alzheimer's disease. *J Anat* 2010; 217(6): 683-93.
65. Rivolta I, Binda A, Molteni L, Rizzi L, Bresciani E, Possenti R, et al. JMV5656, a novel derivative of TLQP-21, triggers the activation of a calcium-dependent potassium outward current in microglial cells. *Front Cell Neurosci* 2017; 11: 41.
66. Lian H, Litvinchuk A, Chiang AC, Aithmitti N, Jankowsky JL, Zheng H. Astrocyte-microglia cross talk through complement activation modulates amyloid pathology in mouse models of Alzheimer's disease. *J Neurosci* 2016; 36(2): 577-89.
67. Ferreira R, Santos T, Viegas M, Cortes L, Bernardino L, Vieira OV, et al. Neuropeptide Y inhibits interleukin-1 β -induced phagocytosis by microglial cells. *J Neuroinflammation* 2011; 8: 169.
68. Y Li, Tan MS, Jiang T, Tan L. Microglia in Alzheimer's disease. *Biomed Res Int* 2014; 2014: 437483.
69. Prodeus AP, Zhou X, Maurer M, Galli SJ, Carroll MC. Impaired mast cell-dependent natural immunity in complement C3-deficient mice. *Nature* 1997; 390(6656): 172-5.

70. Rupprecht TA, Angele B, Klein M, Heesemann J, Pfister HW, Botto M, et al. Complement C1q and C3 are critical for the innate immune response to *Streptococcus pneumoniae* in the central nervous system. *J Immunol* 2007; 178(3): 1861-9.
71. Stevens B, Allen NJ, Vazquez LE, Howell GR, Christopherson KS, Nouri N, et al. The classical complement cascade mediates CNS synapse elimination. *Cell* 2007; 131(6): 1164-78.
72. Shinjyo N, Ståhlberg A, Dragunow M, Pekny M, Pekna M. Complement-derived anaphylatoxin C3a regulates in vitro differentiation and migration of neural progenitor cells. *Stem Cells* 2009; 27(11): 2824-32.
73. Kisselev AF, van der Linden WA, Overkleeft HS. Proteasome inhibitors: an expanding army attacking a unique target. *Chem Biol* 2012; 19(1): 99-115.
74. Yoshimori T, Yamamoto A, Moriyama Y, Futai M, Tashiro Y. Bafilomycin A1, a specific inhibitor of vascular-type H(+)-ATPase, inhibits acidification and protein degradation in lysosomes of cultured cells. *J Biol Chem* 1991; 266(26): 17707-12.
75. Mauvezin C, Neufeld TP. Bafilomycin A1 disrupts autophagic flux by inhibiting both V-ATPase-dependent acidification and Ca-P60A/SERCA-dependent autophagosome-lysosome fusion. *Autophagy* 2015; 11(8): 1437-8.
76. Cho MH, Cho K, Kang HJ, Jeon EY, Kim HS, Kwon HJ, et al. Autophagy in microglia degrades extracellular β -amyloid fibrils and regulates the NLRP3 inflammasome. *Autophagy* 2014; 10(10): 1761-75.
77. Klionsky DJ. Autophagy revisited: a conversation with Christian de Duve. *Autophagy* 2008; 4(6): 740-3.
78. Kirkin V, McEwan DG, Novak I, Dikic I. A role for ubiquitin in selective autophagy. *Mol Cell* 2009; 34: 259-269.
79. Pankiv S, Clausen TH, Lamark T, Brech A, Bruun JA, Outzen H, et al. p62/SQSTM1 binds directly to ATG8/LC3 to facilitate degradation of ubiquitinated protein aggregates by autophagy. *J Biol Chem* 2007; 282: 24121-24145.
80. Mizushima N, Yoshimori T. How to interpret LC3 immunoblotting. *Autophagy* 2007; 3(6): 542-5.
81. Kim J, Kundu M, Viollet B, Guan KL. AMPK and mTOR regulate autophagy through

direct phosphorylation of Ulk1. *Nat Cell Biol* 2011; 13(2): 132-41.

82. Button RW, Vincent JH, Strang CJ, Luo S. Dual PI-3 kinase/mTOR inhibition impairs autophagy flux and induces cell death independent of apoptosis and necroptosis. *Oncotarget* 2016; 7(5): 5157-75.

TLQP-21의 미세아교세포 C3a 수용체 (C3AR1)를 매개로 한 베타-아밀로이드 섭취의 촉진

울산대학교 일반대학원

의학과 의과학전공

장유진

알츠하이머 질병에서 보여지는 베타 아밀로이드 밀집 현상은 그것의 과도한 생성 혹은 미세아교세포, 성상교세포와 같은 교세포를 통한 제거기전의 손상에 의해 나타난다. 미세아교세포는 중추신경계에서 중요한 보호기전을 가지며, 현재 미세아교세포의 베타 아밀로이드 섭취작용을 향상시키는 효과적인 물질을 찾고자 연구되고 있다. Granin family에 속하는 신경펩타이드인 VGF는 단백질 분해효소들에 의하여 여러 종류의 VGF 유래 펩티드들로 절단되는 전구단백질이며, VGF 유래 펩티드 중 하나인 TLQP-21은 미세아교세포 내에서 Ca^{2+} 의 양을 증가시킨다고 보고되어 있다. 이는 TLQP-21이 미세아교세포를 자극하여 기능까지 변조시킬 가능성을 시사한다. 그러나 그러한 TLQP-21로 인한 미세아교세포의 기능적 변조 혹은 알츠하이머 질병과 연관성에 대해서는 밝혀지지 않았다.

본 연구에서는 TLQP-21이 미세아교세포의 섭취작용을 향상시키는 것을 확인하였으며, C3AR1 의존적으로 베타-아밀로이드의 섭취 또한 촉진시킨다. TLQP-21은 미세아교세포의 리소좀의 단백질 제거기전을 향상시킴으로써 섭취한 베타-아밀로이드를 소화를 촉진시키고, 결과적으로 미세아교세포의 베타-아밀로이드 제거 능력을 향상시킨다. 이러한 TLQP-21의 미세아교세포에 미치는 영향들에도 불구하고, TLQP-21은 뇌 내에서 일어나는 염증반응과 관련된 사이토카인의 생산에는 관여하지 않았다. 따라서, TLQP-21은 미세아교세포가 베타 아밀로이드를 제거하는 것을 돕고, 이에 따라서 TLQP-21은 알츠하이머 질병의 새로운 치료제가 될 수 있을 것이다.